Journal of Photochemistry & Photobiology, A: Chemistry 430 (2022) 113954

Contents lists available at ScienceDirect

Journal of Photochemistry & Photobiology, A: Chemistry

journal homepage: www.elsevier.com/locate/jphotochem

Spectral dependence of UV light penetration into powder TiO_2 anatase

Ruslan V. Mikhaylov [a,b,*], Polina E. Lavrik [a,b], Vyacheslav N. Kuznetsov [a,b], Nadezhda I. Glazkova [b]

[a] Saint-Petersburg University, Department of Photonics, Russia
[b] Saint-Petersburg University, Laboratory "Photoactive Nanocomposite Materials", Russia

ARTICLE INFO

Keywords:
Titanium dioxide
Hombifine N
Oxygen isotope exchange
TPD of oxygen
Light penetration depth

ABSTRACT

The penetration depth of UV monochromatic light into deposited TiO_2 anatase powder was investigated. The light penetration depth was considered in units of numbers of surface hole, N_s, and electron, N_{O2}, centers activated during irradiation. The numbers of hole centers N_s were obtained from photostimulated oxygen isotope exchange reaction registered by means of mass spectrometry. The numbers of electron centers N_{O2} were obtained from subsequent thermo-programmed desorption spectroscopy of photoadsorbed oxygen O_2^-. It was shown that the depth D of UV light penetration into UV absorbing TiO_2 powder coat depends on the wavelength and intensity I_0 of incident UV light and obeys to the equation $D(I_0) = \frac{1}{k_{eff}} \lg(I_0/I_m)$ obtained from the Beer–Lambert–Bouguer law with effective extinction coefficient k_{eff} and minimal value of light intensity I_m, below which the photoactivation is considered negligible. Commonly, the value I_m has an order of a few microwatts/cm^2 for activation of electron and hole type centers except for a case of 334 nm falling into the band of the first direct band-to-band transition of anatase, where relatively high threshold value I_m=0.063 mW/cm^2 for photoactivation of hole centers was revealed. Effective extinction coefficient k_{eff} may be considered proportional to the absorption coefficient of TiO_2 in the region of fundamental absorption, whereas, in the non-fundamental absorption region, k_{eff} exceeds significantly that of TiO_2 due to, probably, dominating scattering processes. At small intensities of the incident light, there is a strong sensitivity of the penetration depth (and activated surface) to the intensity.

1. Introduction

Investigation of titanium dioxide and TiO_2-based materials is widely popular because titania is believed to be a perspective material for photocatalytic application under irradiation in UV region [1 –4]. New generations of TiO_2 based materials either doped with various metal and non-metal elements or placed into various heterostructures have been widely investigated during the last two decades due to enhanced absorption in the visible spectral range of such objects that are considered perspective from the standpoint of expanding the spectral range of activation of TiO_2-based photocatalysts to the visible range [3,4]. The comparison of activities of both pure and modified materials, as well as an investigation of the nature of raising/decreasing activity caused by any modification, should be based on the spectral dependences of photostimulated reaction rate. Any investigation of spectral properties of photocatalysts requires monochromatic light varied in a wide spectral range, including the range of fundamental and non-fundamental light absorption of solid. In this relation, one must have such a sample with such thickness that provides the trustworthy registration of photoreaction rates under monochromatic light in the whole spectral region used.

Crystals and dense crystalline or polycrystalline films have specific geometrical dimensions and a permanent surface for reactions (coinciding with the geometric area), and the total photoactivity towards the photoreactions is rather determined by the processes of photogeneration of charge carriers in the bulk and diffusion of them to the surface with subsequent localization. Obviously, the depth of light penetration into crystals (or films) depends on the light absorption coefficient $k(\lambda)$. It determines only the region of the bulk $d=1/k(\lambda)$, where charge carrier generation occurs, and observed surface activity depends roughly on the mean free paths of carriers and their concentration. In any case, there is the constant value of surface and, consequently, some surface centers able to be activated may be taken as a constant value in further considerations.

Powders are not such ideal objects for investigations. Particles

* Corresponding author.
E-mail addresses: ruslan1978@mail.ru, ruslan.mikhaylov@spbu.ru (R.V. Mikhaylov).

https://doi.org/10.1016/j.jphotochem.2022.113954
Received 27 December 2021; Received in revised form 24 March 2022; Accepted 9 April 2022
Available online 12 April 2022

forming the powder have dimensions comparable to or less than the light wavelength. Light absorption is accompanied by the scattering process, which in turn depends on particle sizes, packing density, the absorption coefficient of material $k(\lambda)$, and the wavelength λ of light. Thus many non-control factors are influencing the light penetration depth [5]. Moreover, the number of layers of irradiated particles (i.e., particles participating in photoreactions) correlates with the light penetration depth, thus making the total surface involved in photoreaction be variable that may play a significant role in the analysis of data and interpretation of results. Such phenomenon may appear in spectral measurements when the light penetration (and activated surface) depends on the absorption coefficients $k(\lambda)$ [5]. Moreover, the depth depends on light intensity in scattering media [6].

Of course, this question is not novel and had been arisen earlier with the aim either to avoid the non-illuminated fraction of catalysts [7] or to irradiate photocatalysts as entirely as possible [8,9]. It is also attractive for theoretical and experimental investigations [10 –16]. The term "critical mass" implies such value of the weight of catalysts the exceeding of which results in emerging the non-illuminated fraction of catalysts [8]. The alternative term "penetration depth" is defined as the depth in a semi-infinite layer where the radiation flux density is reduced either to 1% of that at the irradiated surface [14] or to some minimal intensity value, I_m, required for photoinduced activity [6]. Apparently, both terms have similar meanings. The maximal permissible thickness (in units of thickness, weight, density, concentration, etc.) of powder, as a rule, is determined by means of measuring the dependence of the rate of photostimulated reaction on the catalysts loading, the point of saturation of which with a sample loading corresponds to this critical value [7,8]. Practically the irradiance condition for estimating the critical value is usually dependent on the type of light sources, which may have continuous, discrete, or combined discrete-continuous spectra in the required region. In most cases, the values of critical weight are determined for either the wide spectral region (polychromatic irradiation) or chosen dominant spectral line(s) falling in the region of fundamental absorption of photocatalysts and for certain light intensity used in measurements. Thus the results obtained may be considered as either integrated over the definite spectral region or reduced to one dominant spectral line. (In the last case, some other low-intensive neighboring lines are often ignored). Generally, this critical value should also depend on the method of powder packing [7–9]. For titania powder placed on the bottom window of the vertical tubular reactor, this value for a polychromatic UV light (λ<400 nm) was determined to be equal ~5 mg/cm^2 [9], while for powder deposited onto the flat surface it was obtained 0.2 mg/cm^2 [16] and 0.3 mg/cm^2 [7] or 0.9 mg/cm^2 for spreaded powder over porous support [8] for the same spectral range. Such masses being calculated to the penetration depth units gave the values from 1 up to 30 μm depending on the powder packing density [7]. Despite some specific critical weight values for TiO_2 having been already obtained, the question, which part of the sample is irradiated, remains actual for powder-based sample in connection with the following reasons.

Firstly, due to the experimental methods' requirements, the powder TiO_2 could not always be formed with a desired critical density. Such case is typical for powder titania samples either put in EPR cell [17], or pressed into a disk for IR measurements [18,19], where the usual weight density for titania is about 20-25 mg/cm^2 and the lower value results in the fragility of the disk, or deposited from liquid suspensions onto the wall of the reactor [20], construction of which by force of destiny may not allow either to deposit such thin layers or to determine the weight of very thin layer with sufficient accuracy.

Secondly, there is mainly information about critical weight for TiO_2 obtained for the wide spectral region of fundamental absorption TiO_2, resulting in some uncertainness which part of this spectral region is more effective (or gives the greater depth of light penetration) and which one is less. The last has principal significance from an engineering standpoint for developing a new photocatalytic system [10,12,14].

Thirdly, there is poor information in the literature about the experimentally measured correlation between the intensity of light and the depth of its penetration except, to the best of our knowledge, the results presented in for non-absorbing scattering media [6].

The present work is aimed to estimate (in arbitrary units) the surface of the deposited layer of TiO_2 (anatase) powder able to be activated by monochromatic light of various intensities in the region of fundamental absorption of TiO_2. An estimation based on measuring both the number of surface oxygen anions O_s^{2-} of TiO_2 participating in photostimulated oxygen isotope exchange (POIE) reaction between TiO_2 and $^{18}O_2$ (an isotope substitution reaction) and the number of oxygen molecules O_2^- photoadsorbed during this irradiation. Both reactions occur by following reactions [20–24]

$$TiO_2(Ti^{4+} + O_s^{2-}) + h\nu \rightarrow Ti^{3+} + O_s^- \quad (1)$$

$$^{18}O_{2,gas} + {}^{16}O_s^- \rightarrow {}^{16}O^{18}O_{gas} + {}^{18}O_s^- \quad (2)$$

$$Ti^{3+} + O_{2,gas} \rightarrow Ti^{4+} + O_2^- \quad (3)$$

Specific surface low-coordinated anions O_s^{2-} and cations Ti^{3+} may act as surface active centers. Earlier it had been shown that the number of titania surface oxygen anions participating in photostimulated isotope exchange is limited, and, for TiO_2 Degussa P25, it is about 2×10^{11} cm^{-2} [20], so the reaction (2) takes a finite time. The kinetic run of reaction (2) was registered by means of mass spectrometry, while the number of O_2^- photoadsorbed on the surface by Eq. (3) was measured by means of thermo-programmed desorption (TPD) spectroscopy. The choice of these reactions is governed by the following facts. Firstly, oxygen does not contaminate the surface and consequently does not influence it. Secondly, products are accumulative and it allows measuring the low values of them in a wide range of both the light intensity and wavelengths. As seen, reaction (2) implies the interaction of oxygen with a hole type center $^{16}O_s^-$ [20,22,24], whereas adsorbed oxygen O_2^- is the result of interaction with an electron type center Ti^{3+} *via* reaction (3) [23]. Undoubtedly, the oxygen anions, O_s^{2-}, able to participate in exchange (2) are distributed uniformly over the sample surface with some density, and only the centers situated in the irradiated layers may be activated by Eq. (1). Thus for each light wavelength and intensity, the total number of activated surface anions N_s, is proportional to the light penetration depth. The same proportionality to the depth must be observed for the number of photoadsorbed oxygen N_{O2} (Eq.3).

2. Experimental technique

An experimental setup analogous to described in [20] was used for mass spectrometric kinetic and temperature programmed desorption (TPD) measurements. The oil-free all-metal setup was constructed in such a way to provide a possibility to analyze the composition of either gas in the reactor with a sample or desorbing products from the sample during heating or irradiation. It has been made from standard stainless steel ultrahigh vacuum (UHV) components (based on Conflat© junctions CF16, CF40) and equipped with a turbo-molecular pumping station (TurboLab 80, Leybold Vacuum) and a few magnetic discharge ion pumps (Gamma Vacuum, 10 L/s) in various sections of the setup. Generally, the setup consists of a few sections: gas preparing section, pre-reactor volume, reactor volume, mass spectrometric section. All sections and their parts are separated by UHV valves. They include membrane-capacity or combined (capacity-Pirani) gauges (Pfeiffer) that allow realizing the various combination of preparing and admission of gas/mixtures into the reactor with high accuracy and reproducibility. Mass spectrometer (MS) is realized on a residual gas analyzer module RGA 100 (Stanford Research System, resolution at 10% level = 200) equipped with an independent magnetic discharge ion pump (Gamma Vacuum, 40 L/s) providing the characteristic time of ion source evacuation < 0.03 s. The mass-spectrometer was calibrated to the flow of

gases used in experiments and all possible products. The standard minimal registered flow value is $0.9x10^{10}$ molecules/s, the linear range of measured flow extends to $1x10^{15}$ molecules/s.

A quartz reactor of cylindrical shape (10 mm in thickness and 35 mm in diameter) connected to the setup via quartz-glass-metal junction was used. The powder sample was deposited on the one cylinder end while the opposite end, made from high-quality optical quartz, served as a window for irradiation of the sample. The reactor is equipped with a heater disk and thermocouple fixed permanently on the reactor side, where the sample is deposited. The reactor volume could be connected to the mass spectrometer either through a leak-valve (Nenion) for analyzing the gas composition in the volume or through the UHV valve for flow-through and TPD measurements. The characteristic time of reactor evacuation through MS ion source is $\tau_r = 4.00\pm0.05$ s. In the same way, the reactor could be connected to the "gas section" (i.e., through either the leak or valve) for admission of gas or organizing the gas flow through the reactor to mass spectrometer. Thereby we could perform adsorption/desorption/reaction measurements in a wide range of gas pressure values working in either the flow-through regime (10^{-5} – 10^{-1} Pa) or the quasi-state regime (10^{-1} – 10^{2} Pa). The pressure in the reactor volume is controlled with a membrane-capacitance manometer (Pfeiffer, pressure range $6.65x10^{-3}$ – 133 Pa). High-purity gases O_2, CO, and isotope enriched gas ^{13}CO, $^{18}O_2$ (Linde Gas, IE > 99 and 87%, correspondingly) were used. Before admission to the sample, gases were additionally purified by low-temperature fractionalizing. The leak-valve was tuned so that pressure decreasing caused by gas sampling to MS during whole kinetic run measurements did not exceed 5 %.

For sample irradiation, a system based on the high-pressure arc lamps Hg(Xe) (1000W, Newport) or Xe (150W, OSRAM HBO), condenser/IR filter system, and MDR-2 monochromator (LOMO, Russia, diffraction grating - 300 grooves/mm, f/2.5) was used. The FHWM of monochromatic lines was about 5 nm, and the intensity of the beam may be varied up to 2 mW/cm^2 at the wavelengths corresponding to xenon emission and up to higher values using the Hg emission line (for example, up to 30 mW/cm^2 at λ=365 nm). A set of standard glass light filters (LOMO, Russia), passing light of the required spectral ranges, was applied for intensity regulation. The light intensity was measured by Nova II Laser Power and Energy Meter equipped with a Photodiode Sensor (Ophir Photonics, Israel).

The fine-structured powder TiO_2 Hombifine N (anatase, S=340 m^2/g) was used as the sample. Before preparing the samples, the TiO_2 powder was annealed in the furnace at 873 K for 3 hours in the air to clean it of organic contamination. Before and after this procedure, the powder was characterized by diffuse reflectance spectroscopy (DRS), BET, XRD, and TEM methods[1]. The annealing results in the decreasing of powder specific surface area to (80±3) m^2/g, and the anatase XRD reflectance peaks became narrow. TEM images indicated that the TiO_2 samples annealed consist of anatase particles having a prism shape (with a square in a cross-section of the prism) with six pronounced faces and well-organized edges. Annealed TiO_2 powder was deposited on the reactor wall from a suspension of isopropanol. After evaporation of isopropanol at room temperature, the samples were heated step-by-step up to 623 K in the airflow to remove isopropanol remains. The TiO_2 samples obtained in this manner present mechanically stable, thin, dense, opaque coat with a deposition density of (20±1) mg/cm^2 and geometric areas of 3.5 cm^2. The thickness of the layer was determined with the microscope to equal 200±20 μm, and the density of the layer was 1.0±0.1 g/cm^3, which is about four times less than that of anatase crystal (~3.9 g/cm^3). After deposition and primary air drying, the reactor was connected to the experimental UHV setup and pumped out. The purification of the samples was performed by annealing in pure oxygen at 66.5 Pa at 723 K (primary) for 2 hours and then at 873 K (finely) for 2 hours with condensation of products (CO_2, H_2O) on the trap cooled with liquid nitrogen and replacement of oxygen every 15 minutes until oxygen consumption ceased. Before each experiment, the sample was annealed in oxygen at 823 K. Such annealing served for restoring the surface isotopic composition after the use of ^{18}O-labeled oxygen and to recover the stoichiometry of sample (if the last occurred). It should be noted that UHV annealing of the samples at 873 K did not result in the appearance of oxygen desorption in TPD after exposure of the sample to oxygen. It means that TiO_2 anatase is not reduced by such treatment in contrast to the behavior of the rutile phase under the same condition [4,20,25].

The main parameter of isotopic exchange, α, describing the ^{18}O fraction in a medium (gas or solid), containing the oxygen atoms ^{18}O and ^{16}O, is calculated by formula [20,26]

$$\alpha = \frac{^{18}O}{^{18}O + {}^{16}O} \tag{4}$$

The heteroexchange oxygen isotope reaction may be observable until there is a difference between gaseous isotope fraction α_g and surface fraction α_s, i.e., $\alpha_g - \alpha_s \neq 0$, and at $t\to\infty$ both fractions aim for some equilibrium value α_e [26]. Assuming that accordingly experimental condition $\alpha_{gas}(t=0)= \alpha_0$ and α_{surf} (t=0)=0 and taking into account that surface center contains one oxygen atom and oxygen molecule is a diatomic molecule, one may write the following equation for constancy of isotope ^{18}O in the "gas-surface" system:

$$2N_g a_0 = 2N_g a_e + N_s a_e \tag{5}$$

where N_g and N_s – the numbers of gas molecules and surface exchangeable anions, correspondingly. Knowing N_g, initial α_0 and obtaining the value of equilibrium α_e fractions from the kinetic run of reaction (2), the number of active surface centers may be calculated as

$$N_s = \frac{2N_g(a_0 - a_e)}{a_e} \tag{6}$$

3. Experimental results and discussions

No oxygen adsorption on the non-irradiated TiO_2 anatase surface was found even after exposition to O_2 at the pressure of 66.5 Pa for a few hours by monometrically and TPD (Figs. 1 and 2), while monochromatic or polychromatic UV irradiation (λ<400 nm) of TiO_2 in oxygen is accompanied by pressure decreasing during the first few hundreds of seconds of irradiation (Fig.1). The maximal pressure decreasing value ΔP_{ads} obtained under irradiation has an order of 0.053Pa (Fig. 1) corresponding to adsorption of 3.0×10^{15} molecules O_2. The oxygen consumed under irradiation was equal to that desorbed in subsequent

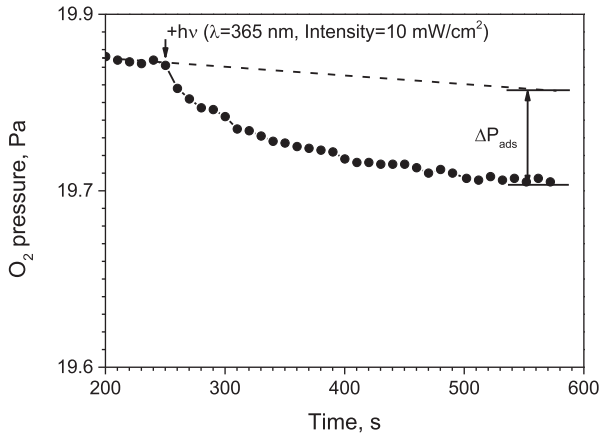

Figure 1. Oxygen pressure changes during dark exposure of TiO_2 to O_2 (dashed line) and under UV illumination in O_2 (line+points). The moment of illumination start marked as "+hν." A slight slope of the pressure curves is due to gas sampling to the mass spectrometer.

[1] See Supplementary Material for details

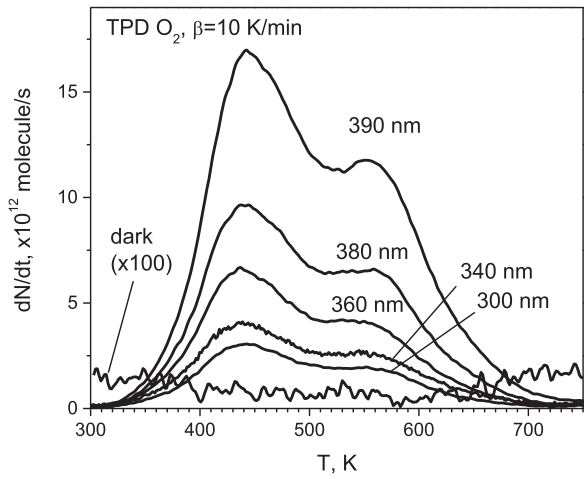

Figure 2. TPD spectra of oxygen after dark exposure for 5 hours (spectrum is multiplied by 100) and irradiation of TiO_2 in 15 Pa of $^{18}O_2$ with monochromatic light of various wavelengths up to saturation in isotope exchange.

TPD spectra. TPD spectra of oxygen photoadsorbed during monochromatic irradiation with various wavelengths are presented in fig. 2. They all are similar in shape and differ only in intensity. The typical oxygen TPD spectrum consists of a few peaks with maxima in the 400-650 K region. Commonly spectra are very similar to the TPD spectrum of O_2 chemosorbed on the reduced surface of TiO_2 P25 [20], indicating the same mechanism of its formation, i.e., via interaction of the gaseous molecule with an electron on the surface (Eq.3).

Irradiation of titania in $^{18}O_2$ is accompanied by an oxygen isotope heteroexchange reaction by Eq. (2). The pressure of $^{18}O_2$ ~16 Pa was enough to provide isotope exchange measurements in a wide range of intensities and wavelengths since the number of gaseous molecules N_g at this pressure was equal to 8.46×10^{17} molecules and exceeded the maximal number of surface exchangeable oxygen anions. The typical kinetic run (for example, the run for the 365 nm wavelength) is presented in fig. 3. It is seen that gaseous isotope fraction $\alpha_g = \alpha_0$ decreases during irradiation aiming to its equilibrium value $\alpha_g = \alpha_e$. Since the POIE rate depends on both intensity and wavelength of light, the reaction runs were recorded during long-term irradiation that usually took from 3 up to 6 hours. For cases of low numbers of exchangeable surface oxygen requiring "short" irradiation times, the equilibrium values of isotope fraction α_e were determined directly from the saturation value of curve $\alpha_g = \alpha_g\,(t)$, which was achieved under irradiation in a reasonable time. For the cases of the significant number of the centers that required

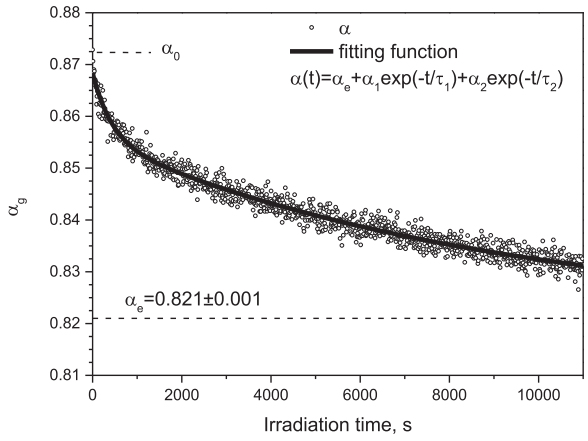

Figure 3. Typical dependence of parameter α_{gas} vs. irradiation time (points) and fitting line by two-exponential decay function (line) (λ=365 nm, Intensity 10 mW/cm^2).

longer irradiation time, the value α_e were obtained from fitting procedure of experimental curve $\alpha_g = \alpha_g(t)$ with two-exponential decay function $\alpha(t) = \alpha_e + \alpha_1 e^{-t/\tau_1} + \alpha_2 e^{-t/\tau_2}$, which had been found to fit well the curves $\alpha_g = \alpha_g(t)$ measured here (fig. 3)[2]. In this case, the irradiation had been being continued until an error of α_e obtained by real-time fitting procedure became lower than an experimental error of α_g determination ($\delta\alpha_g = 0.002$). The numbers of exchangeable oxygen anions N_s were calculated by the formula (6). After each isotope exchange reaction, the TPD measurement was made from which the number of photoadsorbed oxygen N_{O2} was calculated. Thus for each combination of the light wavelength and intensity, the pair of points {N_s; N_{O2}} was obtained.

Fig. 4 presents the dependences of the numbers of activated centers N_s and the number of photoadsorbed oxygen (N_{O2}) on the wavelength λ at the intensity of light 0.4-0.6 mW/cm^2. The left and right scales correspond to N_s and N_{O2}, and it is seen that in the UV region (λ< 390 nm), both curves are synchronic, with a coefficient of $N_s/N_{O2} \approx 45$ between them. The coincidence of the curves on fig. 4 in the fundamental region is obvious because it is a region of electron-hole pairs generation. It is better to present data from graph 4 as N_{O2} *vs.* N_s (fig. 5), where the correlation is seen clearly. It is obvious that there are three branches of distribution of the points. The pairs of points belonging to the spectral region of TiO_2 fundamental absorption (300 – 390 nm) form a straight line (I) with a slope equal to 0.022 (1/0.022=45). The points from the near absorption edge (400-410 nm) organize a transition area (II), and the 420-450 nm region gives point pairs falling in a separate branch (III). The behavior of the both curves N_s and N_{O2} (Fig.4) in the region of fundamental absorption of TiO_2 indicates that as the wavelength decreases, the depth of light penetration in this region reduces due to light absorption coefficient enhancement.

The reason of difference in orders of values N_s and N_{O2} is apparent. When we measure the number of surface hole centers N_s by means of POIE reaction by Eq. (2), we do determine all centers, because in result

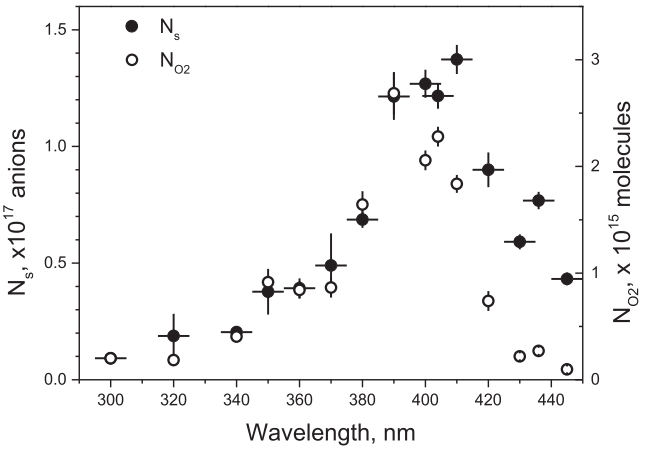

Figure 4. Dependence of the numbers of photoactivated surface anions N_s (left scale, dark circles) and photoadsorbed oxygen N_{O2} (right scale, open circles) on the wavelength of light at the light intensity of 0.4-0.6 mW/cm^2.

[2] Applying the two-exponential decay function (instead of the one-exponential one $\alpha(t) = \alpha_e + (\alpha_0 - \alpha_e)\exp\left\{-\frac{R}{N_g}\left(1+\frac{2N_g}{N_s}\right)t\right\}$ as it is expected [26]) for curve α(t) fitting is caused either by the presence of two (or more) types of exchangeable centers (N_{s1}, N_{s2}) on the surface, or by rate *R* decreasing during irradiation (or due to some reasons else). The solution for each particular case requires numerical calculations and individual consideration. The equilibrium value α_e is anyway determined by equation (5), assuming $N_s = N_{s1} + N_{s2}$, and it is independent on the exchange rate.

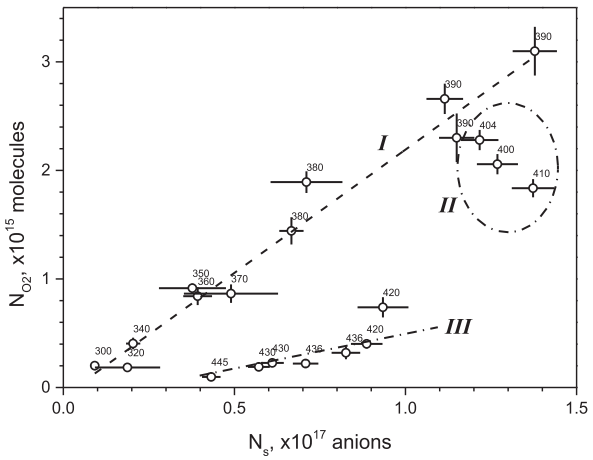

Figure 5. Correlation between the numbers of photoactivated surface anions N_s (X-scale) and photoadsorbed oxygen N_{O2} (Y-scale) measured at the various wavelength of light at the constant light intensity of 0.4-0.6 mW/cm^2.

of reaction (2) no destruction of centers as well as no charge accumulation on the surface occur. Any processes of electron-hole recombination also do not influence this result. At the same time the number of photoadsorbed oxygen species N_{O2} is only proportional to all possible surface electron centers, because photoadsorption of oxygen is saturated due to accumulation of negative charge on the surface by Eq. (3), which reduces the rate of oxygen adsorption and then prevents it totally. Also, the presence of O_2^- on the surface initiates the competing route of photogenerated hole consumption for O_2^- desorption by scheme

$$O_2^- + h \rightarrow O_2\uparrow \quad (7)$$

This was seen very well at low (1.3×10^{-3} – 1.3×10^{-4} Pa) pressures of oxygen by replacing of gaseous $^{18}O_2$ by $^{16}O_2$ and had been observed by us earlier on TiO_2 Degussa P-25 [20]. As result there is a certain coverage of adsorbed oxygen O_2^- forming on the surface by means of processes, described by Eqs. (3) and (7). It is worth noting that at higher pressure of oxygen (P>10^{-1} Pa) the rate of process 7 is much less than that of process 3 and oxygen photodesorption could be considered negligible. Thus, the amount of adsorbed oxygen N_{O2} can be considered only proportional to the number of electronic centers and, at the same time, also proportional to the irradiated surface.

In the visible region (λ> 390 nm), both dependences N_s and N_{O2} are non-zero (and even comparable with those in the UV region) indicating the possibility of photoactivation in this spectral region (Figs. 4, 5), although the POIE rates in this region are too low. This region of absorption belongs to the non-fundamental one and is usually associated with absorption by defects. The curve N_{O2} diverges from N_s (Fig. 4), indicating the various spectral features of photoexciting of a few types of defects (electron donors and hole donors) each of which is responsible for activation either electron or hole type centers. This region is non-absorbing (or weakly absorbing), so the light penetration depth may be expected to have greater values than in UV region, but, on the other hand, intense scattering may reduce the depth to the values observed. The second factor, complicating the consideration, is that the amounts of defects are limited, thus leading to the saturation of activation due to total ionization of available states. The last may be rather applied to the donor of electrons, because electrons are captured on the surface by Eq. (3)., thus remaining a part of donors in ionized state. As to hole donors, they may be considered as renewing, because the reaction (2) is not accompanied by hole capturing. If the last reason is assumed and the effect of scattering is dominant, one may consider the points N_s at λ> 390 nm on fig. 4 indicative of the spectral profile of light penetration depth at the intensity of 0.4-0.6 mW/cm^2 in this region.

For example, let us look at the spectral dependence of CO uptake rate in photooxidation reaction CO+O_2+hν measured at the same light intensity of 0.4-0.6 mW/cm^2 (Fig. 6). The reaction of CO uptake occurs due to the interaction of the gaseous CO with the hole centers O_s^- [19]. It is seen that the dependence has a maximum at λ= 370-380 nm and, as the wavelength decreases to 300 nm, it declines identically to the curve N_s *vs.* λ presented in Fig. 4. Apparently, this decline is caused by the active surface decreasing than any spectral features of TiO_2 excitation. Moreover, the maximum observed in Fig. 6 may be just a result of convolution of the authentic spectral curve of activation and the curve of the light penetration depth.

For measurements of light penetration depth on the light intensity, a few UV mercury spectral lines of Hg(Xe) arc lamp (1000W) were used, the intensities of which were higher than the intensity of the continuous spectrum of the Xe component in the UV range. It allowed varying the intensities in a wide range.

The dependencies on intensity I_0 of N_s (proportional to the light penetration depths) measured at the wavelengths 303, 334, 365, 390, 404 nm are presented in Fig. 7. It is seen that all dependencies have a similar form characterized by a sharp increase in the range of low intensities (0…1 mW/cm^2) with subsequent sloping parts at higher values. An apparent consequence is that the light penetration depth is sensitive very much to an intensity deviation in the region of low intensities (for this case, it is 0…1 mW/cm^2), which may result in enhanced fluctuation during measurement of the reaction rates in this intensity region due to involving (or excluding) of some part of the surface into reaction. Suppose such a phenomenon should be considered when planning the measurements and estimating a measurement error. Moreover, the results obtained here show that even using monochromatic light of the same wavelength, but of different intensity, to irradiate the powder, we must keep in mind that the number of active centers that can be involved in the reaction is not constant, but depends on the intensity. This plays an important role in the analysis of kinetic data, in the determination of rate constants, interaction cross-sections, in the construction of models and theories.

The curves drown as N_s, and N_{O2} *vs.* lg(I_0) represent straight lines (Fig. 8A and 8B), which may be well fitted with an equation

$$N(I_0) = \frac{1}{k_{eff}}\lg\left(\frac{I_0}{I_m}\right) = \frac{1}{k_{eff}}\lg(I_0) - \frac{1}{k_{eff}}\lg(I_m) \quad (8)$$

that is obtained from the Beer–Lambert–Bouguer law for the depth (corresponding to N_s and N_{O2}) at which intensity becomes equal to an intensity I_m [6]. The value I_m may be considered an intensity at which reactions on the surface are not initiated or become undetectable [6].

The main result of such approximation is that the penetration of light, the spectral region of which coincides with fundamental

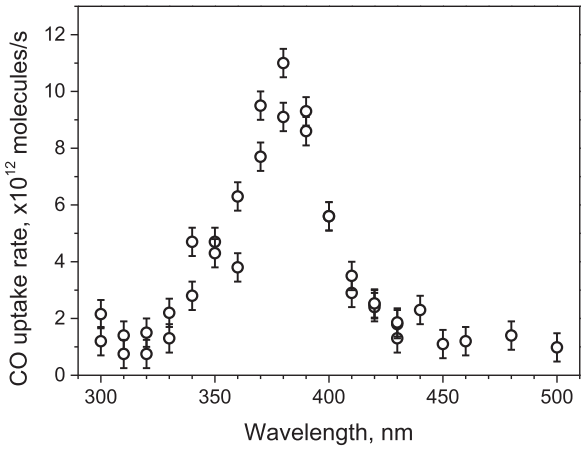

Figure 6. Spectral dependences of CO uptake rate in photooxidation reaction CO+O_2+hν on the TiO_2 sample at the light intensity of 0.4-0.6 mW/cm^2 measured in flow (2.5×10^{14} molecules/s) of the mixture of CO:O_2=1:1.

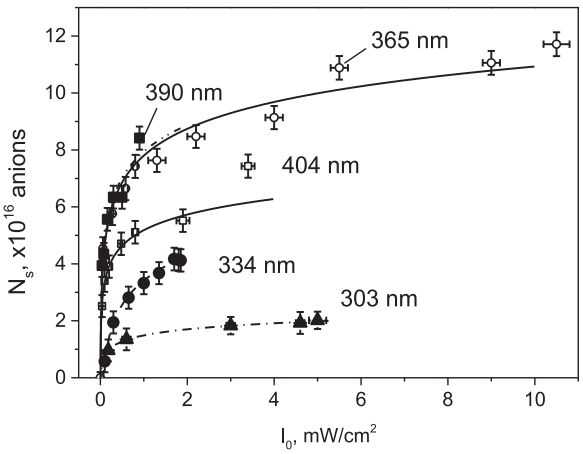

Figure 7. The dependences of substituted oxygen N_s on light intensity I_0 for various monochromatic irradiation.

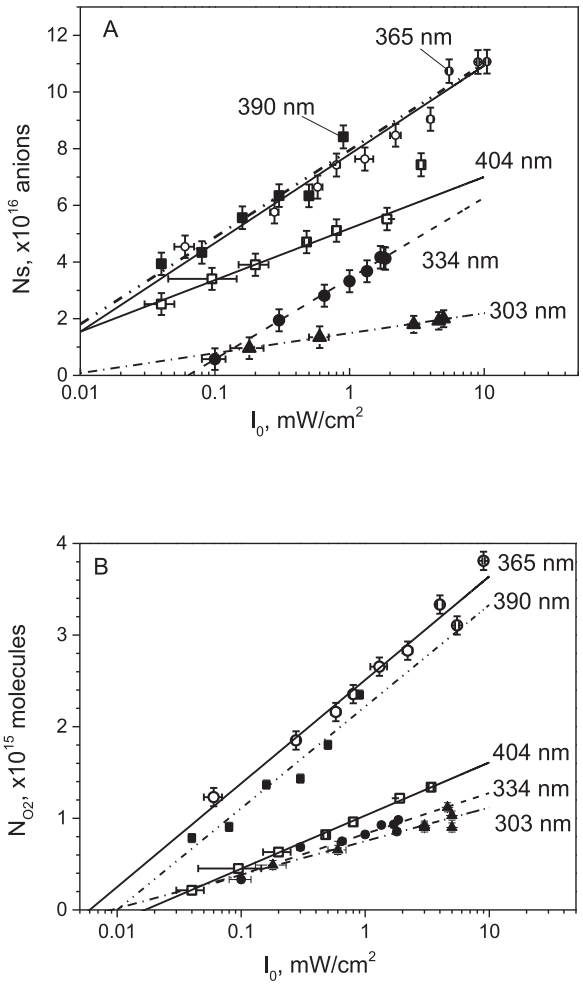

Figure 8. The dependences N_s (A) and N_{O2} (B) *vs.* lgI_0.

absorption of powder, may be considered in the framework of the Beer–Lambert–Bouguer law using some effective value k_{eff}. The same results were obtained for ceramic membranes [11]. In this case, the value of effective extinction coefficient k_{eff} is not equal to the absorption coefficient of crystal and probably may include some other parameters (scattering, density, etc.) [6], which make it differ from that of crystal. The values of k_{eff} and I_m obtained by fitting procedure with eq. (8) for each dependence are presented in Table 1.

Fig. 9 demonstrates both the Kubelka-Munk transformation of the diffuse reflection spectrum of the powder TiO_2 Hombifine N diluted in MgO powder (5% wt.) and parameters $k_{eff}(\lambda)$ presented in Table 1. The K-M function of diluted TiO_2 powder may be considered proportional to the absorption coefficient of TiO_2 in the region of fundamental absorption [27,28].

It is seen from fig. 9 that k_{eff} obtained from N_{O2} curves is close to the K-M function f_{KM} in the region of fundamental absorption. In the region of fundamental absorption of anatase the absorption of light may be considered as a dominant route of its disappearance during penetration into the sample. In contrast to UV region, the 390 and 404 nm points differ from f_{KM}. As it was said above, these points are falling into non-fundamental region of anatase absorption which may be due to the shallow states of defects. These defects could be assigned to the local absorption centers distributed in scattering matrix of TiO_2 transparent at λ>380 nm. Thus, the dominant route in this case is scattering process that prevents penetration of light deep into the sample. In framework of application of term "the absorption coefficient" it looks like increase in its value (although this does not correspond to reality), thus it was better to use the term "the effective extinction coefficient" which is proportional to the real absorption coefficient in the case of strong absorption and may differ in other case. Of course, it is better to apply this term to powders (or turbid medium) only.

At the same time, dependence k_{eff} *vs.* λ obtained from N_s curves differs significantly from the K-M function at λ=334 nm. As for this point, an interesting feature could be noted from a set of curves drown on figs 8A and 8B as well as from Table 1. The behavior of the curve N_s obtained for the 334 nm line drops out the behaviors of other lines in Fig. 8A and does not coincide with the curve N_{O2} at the same wavelength (fig. 8B). It is seen that in the semi-logarithm plot, the 334 nm's straight line has the same slope as the lines for 365 and 390 nm (it looks like it shifted downwards), but its intercept differs significantly. From equation (7), the intercept is related to such value of light intensity I_m, which does not induce any processes (or induce non-detectable ones). For all other spectral lines, the value I_m is about a few microwatts/cm^2, whereas the line 334 nm is characterized by the higher value of threshold intensity $I_m = 0.063$ mW/cm^2 (Table 1). So high value of non-active intensity is accompanied by decreasing the penetration depth for excitation of hole type centers. In contrast, the electron type centers at this wavelength are probably activated at larger depths. The wavelength 334 nm ($h\nu$ = 3.71 eV) falls into the first band of direct band-to-band transition for **E⊥c** of pristine and n-doped anatase crystals, maximum of which accordingly to spectroscopic ellipsometry is equal to 3.79 eV [29]. Excitation in the band of direct band-to-band transition may be accompanied by enhanced recombination resulting in a low yield of photoactivation of the surface hole centers and/or appearance of competing for the route of energy consumption (for example, the generation of excitons [29]). In any case, the data obtained here, as well as methods used, do not allow speculating more, so let us remain an investigation of this feature for the future.

Table 1
Values of k_{eff} and I_m calculated from the linear fit function by eq.8 for N_s and N_{O2} dependences on light intensity I_0, presented in fig. 8 a and b.

λ, nm	Ns dependences k_{eff}, anions^{-1} (*)	I_m, μW/cm^2	N_{O2} dependences k_{eff}, molecules^{-1} (*)	I_m, μW/cm^2
303	(1.42±0.18)×10^{-16}	7±5	(2.72±0.41)×10^{-15}	9±7
334	(3.49±0.09)×10^{-17}	63±4	(2.25±0.25)×10^{-15}	14±7
365	(3.19±0.33)×10^{-17}	3±2	(8.82±0.59)×10^{-16}	6±2
390	(3.25±0.46)×10^{-17}	3±2	(9.0±1.2)×10^{-16}	10±6
404	(5.50±0.30)×10^{-17}	1.4±0.5	(1.72±0.03)×10^{-15}	16±1

* Units and orders of k_{eff} values are caused by these of N_s and N_{O2} used in eq.8

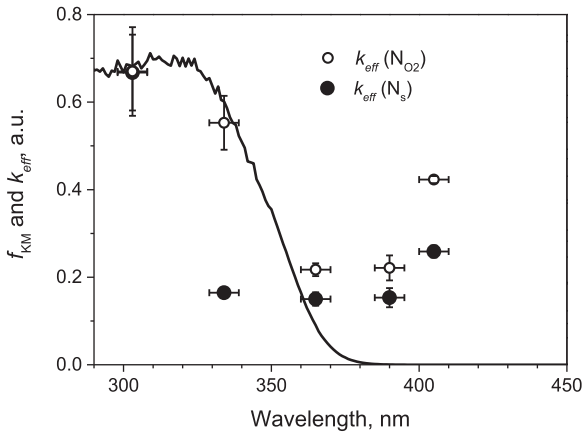

Figure 9. The Kubelka-Munk transformation (the K-M function f_{KM}) of diffuse reflectance spectra of the TiO_2 Hombifine N powder diluted (5 % wt.) in MgO powder (line) and coefficients k_{eff} of fitting of the curves on fig. 7 by eq. (8) (points).

4. Conclusions

By means of photostimulated oxygen isotope exchange reaction and TPD measurements of photoadsorbed oxygen, the numbers of activated surface centers of the deposited coat of TiO_2 powder were obtained at various wavelengths and intensities of incident UV light. Assuming the direct proportionality between the number of the activated centers and light penetration depth (or activated surface), it was shown that the depth of UV light penetration into UV absorbing TiO_2 powder coat depends on the wavelength and intensity of incident UV light. The penetration of light into a strongly absorbing TiO_2 powder sample may be considered in the framework of the Beer–Lambert–Bouguer law with effective extinction coefficient k_{eff} which is proportional to the absorption coefficient of crystal $k(\lambda)$ in UV region ($\lambda<380$ nm), while for VIS light ($\lambda>380$nm) the value k_{eff} differs from $k(\lambda)$ probably due to dominating of scattering component. It was shown that at relatively small intensities of the incident light, there is a strong sensitivity of the penetration depth to the intensity. The relatively high threshold intensity (0.063 ± 0.004 mW/cm^2) for photoactivation of hole centers was found at the irradiation wavelength 334 nm, falling into the band of the first direct band-to-band transition of anatase.

CRediT authorship contribution statement

Ruslan V. Mikhaylov: Conceptualization, Funding Aquisition, Data curation, Writing (all), Vizualization, Investigation, Validation, Formal Analysis, Methodology, Supervizion, Resources, Project administration. **Polina E. Lavrik:** Data curation, Writing – original draft, Investigation. **Vyacheslav N. Kuznetsov:** Conceptualization, Investigation, Validation, Methodology. **Nadezhda I. Glazkova:** Data curation, Writing – original draft, Investigation.

Declaration of Competing Interest

The authors declare that they have no known competing financial interests or personal relationships that could have appeared to influence the work reported in this paper.

Acknowledgments

The reported study was funded by RFBR according to the research project № 19-02-00749. Authors are grateful to Saint-Petersburg State University (PureID 73032813) and to the Resource Centers "Nanophotonics", "Centre for X-ray diffraction Studies", "Centre for Innovative Technologies of Composite Nanomaterials" and "Nanotechnology" of Saint-Petersburg State University for the sample characterization by means of DRS, XRD, BET, and TEM measurements.

Appendix A. Supplementary data

Supplementary data to this article can be found online at https://doi.org/10.1016/j.jphotochem.2022.113954.

References

[1] A. Linsebigler, G. Lu, J. Yates Jr., Photocatalysis on TiO_2 surfaces: principles, mechanisms, and selected results, Chem. Rev. 95 (1995) 735–758, https://doi.org/10.1021/cr00035a013.
[2] U. Diebold, The surface science of titanium dioxide, Surf. Sci. Rep. 48 (2003) 53–229, https://doi.org/10.1016/S0167-5729(02)00100-0.
[3] A. Fujishima, X. Zhang, D.A. Tryk, TiO_2 photocatalysis and related surface phenomena, Surf. Sci. Rep. 63 (2008) 515–582, https://doi.org/10.1016/j.surfrep.2008.10.001.
[4] M.A. Henderson, A surface science perspective on TiO_2 photocatalysis, Surf. Sci. Rep. 66 (2011) 185–297, https://doi.org/10.1016/j.surfrep.2011.01.001.
[5] T.A. Egerton, UV-Absorption—The Primary Process in Photocatalysis and Some Practical Consequences, Molecules 19 (2014) 18192–18214, https://doi.org/10.3390/molecules191118192.
[6] M.L. Griffith, J.W. Halloran, Scattering of ultraviolet radiation in turbid suspensions, J. Appl. Phys. 81 (1997) 2538–2546, https://doi.org/10.1063/1.364311.
[7] W.A. Jacoby, D.M. Blake, R.D. Noble, C.A. Coval, Kinetics of the oxidation of trichloroethylene in air via heterogeneous photocatalysis, J. Catal. 157 (1995) 87–96, https://doi.org/10.1006/jcat.1995.1270.
[8] M. Formenti, F. Juillet, P. Meriaudeau, S.J. Teichner, P. Vergnon, Preparation in a hydrogen-oxygen flame of ultrafine metal oxide particles. Oxidative properties toward hydrocarbons in the presence of ultraviolet radiation, J. Colloid Interface Sci. 39 (1972) 79–89, https://doi.org/10.1016/0021-9797(72)90144-0.
[9] W. Mu, J.-M. Herrmann, P. Pichat, Room temperature photocatalytic oxidation of liquid cyclohexane into cyclohexanone over neat and modified TiO_2, Catal. Lett. 3 (1989) 73–84, 10.1007%2FBF00765057.
[10] M.B. van der Mark, M.P. van Albada, A. Lagendijk, Light scattering in strongly scattering media: Multiple scattering and weak localization, Phys. Rev. B 37 (1988) 3575–3592, https://doi.org/10.1103/PhysRevB.37.3575.
[11] M.A. Aguado, M.A. Anderson, C.G. Hill Jr., Influence of light intensity and membrane properties on the photocatalytic degradation of formic acid over $Ti0_2$ ceramic membranes, J. Mol. Catal. 89 (1994) 165–178, https://doi.org/10.1016/0304-5102(93)E0282-L.
[12] O.M. Alfano, M.I. Cabrera, A.E. Cassano, Modeling of light scattering in photochemical reactors, Chem. Eng. Sci. 49 (1994) 5327–5346, https://doi.org/10.1016/0009-2509(94)00288-6.
[13] W.E. Vargas, G.A. Niklasson, Intensity of diffuse radiation in particulate media, J. Opt. Soc. Am. A 14 (1997) 2253–2262, https://doi.org/10.1364/JOSAA.14.002253.
[14] A. Ciani, K.-U. Goss, R.P. Schwarzenbach, Light penetration in soil and particulate minerals, Eur. J. Soil Sci. 56 (2005) 561–574, https://doi.org/10.1111/j.1365-2389.2005.00688.x.
[15] D. Oelkrug, M. Brun, K. Rebner, B. Boldrini, R. Kessler, Penetration of Light into Multiple Scattering Media: Model Calculations and Reflectance Experiments. Part I: The Axial Transfer, Appl. Spectrosc. 66 (8) (2012) 934–943.
[16] W. Choi, S.J. Hong, Y.-S. Chang, Y. Cho, Photocatalytic Degradation of Polychlorinated Dibenzo-p-dioxins on TiO_2 Film under UV or Solar Light Irradiation, Environ. Sci. Technol. 34 (22) (2000) 4810–4815, https://doi.org/10.1021/es0011461.
[17] T. Berger, O. Diwald, E. Knozinger, M. Sterrer, J.T. Yates Jr., UV induced local heating effects in TiO_2 nanocrystals, Phys. Chem. Chem. Phys. 8 (2006) 1822–1826, https://doi.org/10.1039/B517107E.
[18] C.N. Rusu, J.T. Yates Jr., Photochemistry of NO Chemisorbed on TiO_2(110) and TiO_2 Powders, J. Phys. Chem. B 104 (2000) 1729–1737, https://doi.org/10.1021/jp992239b.
[19] R.V. Mikhaylov, A.A. Lisachenko, B.N. Shelimov, V.B. Kazansky, G. Martra, G. Alberto, S. Coluccia, FTIR and TPD analysis of surface species on a TiO_2 photocatalyst exposed to NO, CO, and NO-CO mixtures: effect of UV–vis light irradiation, J. Phys. Chem. C 113 (2009) 20381–20387, https://doi.org/10.1021/jp906176c.
[20] R.V. Mikhaylov, A.A. Lisachenko, V.V. Titov, Investigation of photostimulated oxygen isotope exchange on TiO_2 Degussa P25 surface upon UV-Vis irradiation, J. Phys. Chem. C 116 (2012) 23332–23341, https://doi.org/10.1021/jp305652p.
[21] R.I. Bickley, F.S. Stone, Photoadsorption and photocatalysis at rutile surfaces: I. Photoadsorption of oxygen, J. Catal. 31 (1973) 389–397, https://doi.org/10.1016/0021-9517(73)90310-2.
[22] H. Courbon, M. Formenti, P. Pichat, Study of oxygen isotopic exchange over ultraviolet irradiated anatase samples and comparison with the photooxidation of isobutane into acetone of Isobutane into Acetone, J. Phys. Chem. 81 (1977) 550–554, https://doi.org/10.1021/j100521a012.
[23] T. Berger, M. Sterrer, O. Diwald, E. Knozinger, Charge trapping and photoadsorption of O_2 on dehydroxylated TiO_2 nanocrystals - An electron

paramagnetic resonance study, ChemPhysChem 6 (2005) 2104–2112, https://doi.org/10.1002/cphc.200500161.
[24] C. Günnemann, D.W. Bahnemann, P.K.J. Robertson, Isotope Effects in Photocatalysis: An Underexplored Issue, ACS Omega 6 (17) (2021) 11113–11121, https://doi.org/10.1021/acsomega.1c00178.
[25] U. Diebold, N. Ruzycki, G.S. Herman, A. Selloni, One step towards bridging the materials gap: surface studies of TiO_2 anatase, Catalysis Today 85 (2003) 93–100, https://doi.org/10.1016/S0920-5861(03)00378-X.
[26] A. Ozaki, Isotopic Studies of Heterogeneous Catalysis, Kodansha Ltd., Tokyo, and Academic Press, New York, 1977.
[27] G. Kortum, Reflectance Spectroscopy: Principles, Methods, Applications, (Translated from the German by J.E. Lohr, Philadelphia), Springer, Berlin, Heidelberg, 1969. Doi: 10.1007/978-3-642-88071-1.
[28] K. Klier, Reflectance Spectroscopy as a Tool for Investigating Dispersed Solids and Their Surfaces, Catal. Rev.-Sci. Eng. 1 (1968) 207–232, https://doi.org/10.1080/01614946808064704.
[29] E. Baldini, L. Chiodo, A. Dominguez, M. Palummo, S. Moser, M. Yazdi-Rizi, G. Auböck, B.P.P. Mallett, H. Berger, A. Magrez, C. Bernhard, M. Grioni, A. Rubio, M. Chergui, Strongly bound excitons in anatase TiO_2 single crystals and nanoparticles, Nat. Commun. 8 (2017) 13, https://doi.org/10.1038/s41467-017-00016-6.